

Expression of SARS-coronavirus envelope protein in *Escherichia coli* cells alters membrane permeability

Y. Liao^a, J. Lescar^a, J.P. Tam^a, D.X. Liu^{a,b,*}

^a School of Biological Science, Nanyang Technological University, 61 Biopolis Drive, Proteos, Singapore 138673, Singapore

^b Institute of Molecular and Cell Biology, 61 Biopolis Drive, Proteos, Singapore 138673, Singapore

Received 27 September 2004

Abstract

To promote viral entry, replication, release, and spread to neighboring cells, many cytolitic animal viruses encode proteins responsible for modification of host cell membrane permeability and for formation of ion channels in host cell membranes during their life cycles. In this study, we show that the envelope (E) protein of severe acute respiratory syndrome-associated coronavirus can induce membrane permeability changes when expressed in *Escherichia coli*. E protein expressed in bacterial and mammalian cells under reducing conditions existed as monomers, but formed homodimer and homotrimer under non-reducing conditions. Site-directed mutagenesis studies revealed that two cysteine residues of the E protein were essential for oligomerization, leading to induction of membrane permeability. This is the first report demonstrating that a coronavirus-encoded protein could modify membrane permeability in *E. coli* cells.

© 2004 Elsevier Inc. All rights reserved.

Keywords: Severe acute respiratory syndrome coronavirus; Envelope protein; Membrane permeability; *Escherichia coli*; E protein; Oligomerization; Viroporin

A novel coronavirus was identified as the causative agent of the recent epidemic of severe acute respiratory syndrome (SARS) [18]. Similar to other coronaviruses, SARS coronavirus (SARS-CoV) is an enveloped virus with a single strand, positive-sense RNA genome of 29.7 kb in length. Upon virus entry into cells, a 3'-coterminally nested set of 9 mRNAs is produced [20]. The genome-length mRNA, mRNA₁, expresses two overlapping replicase proteins in the form of polyproteins 1a and 1a/b. The polyproteins are subsequently processed into at least 16 putative nonstructural proteins (NSP1–NSP16) by virus-encoded proteinases [20]. The mature proteins comprise proteinases, RNA-dependent RNA polymerase, and helicase, involved in the genomic and subgenomic RNA synthesis. The four

structural proteins, arranged in the order 5'-S-E-M-N-3', are encoded by subgenomic mRNA 2, 4, 5, and 9, respectively. In addition, eight putative nonstructural proteins, 3a, 3b, 6, 7a, 7b, 8a, 8b, and 9b, are encoded by mRNA₃, 6, 7, 8, and 9, respectively [20]. They are unique proteins of SARS-CoV and very little is known about the functions of these nonstructural proteins [18,20].

Coronavirus infection of cultured cells causes typical cytopathic effects (CPEs), including rounding-up and fusion of the infected cells, detachment of cells from the culture dishes, cell lysis, and death [13]. Among them, formation of giant syncytial cells is the hallmark of early CPE in cells infected with most coronaviruses. The prominent CPE in cells infected with SARS-CoV, however, is rounding up of the infected cells, cell detachment, and lysis [9]. Typically, two types of membrane active proteins are able to modify membrane

* Corresponding author. Fax: +65 67791117.

E-mail address: dxliu@imcb.a-star.edu.sg (D.X. Liu).

permeability, leading to lysis of virus-infected cells [4,7]. The first type of these membrane active proteins is the viral proteins with fusogenic activity. One example of such proteins is the hepatitis C virus (HCV) E1 protein [5]. The second type is a group of small, hydrophobic proteins termed viroporins [4,7].

Viroporins are small, highly hydrophobic viral proteins that could interact with cellular membranes and modify membrane permeability to ions or other small molecules. In this manner, viroporins disorganize the membrane, cause cell lysis, and facilitate the release of viral progeny. This group of viral proteins is usually expressed at late stages of the infection cycles, forming hydrophilic pores in the plasma membrane and inducing a general increase in permeability to ions and small molecules, but not to macromolecules [4,7]. Viroporins have been found in many viruses, such as HCV p7 protein [8,15], human immunodeficiency virus type 1 (HIV-1) Vpu [6], influenza A virus M2 [16], hepatitis A virus 2B [10], Semliki Forest virus 6K [19], picornavirus 2B [1,2,11], and avian reovirus p10 protein [3].

In this study, we aimed to identify and characterize SARS-CoV proteins that may induce membrane permeability upon expression in bacterial cells. Among five proteins tested, the E protein can obviously enhance membrane permeability to *o*-nitrophenyl- β -D-galactopyranoside (ONPG), a β -galactosidase substrate, and hygromycin B (HB), an antibiotic which can inhibit protein synthesis. Analysis of the E protein expressed in bacterial and mammalian cells demonstrated that the protein may form homodimer and homotrimer, and site-directed mutagenesis studies revealed that two cysteine residues of the E protein located at amino acid positions 40 and 44 are essential for the formation of oligomers and for induction of membrane permeability in *Escherichia coli* cells. These results together with the predicted structural similarity with known membrane-permeable proteins of other viruses suggest that the E protein might be a putative viroporin.

Experimental procedures

Transient expression of SARS-CoV sequence in mammalian cells. HeLa cells were grown at 37 °C in 5% CO₂ and maintained in Glasgow's modified Eagle's medium supplemented with 10% fetal calf serum.

SARS-CoV sequences were placed under the control of a T7 promoter and transiently expressed in mammalian cells using a vaccinia virus-T7 expression system. Briefly, 60–80% confluent monolayers of HeLa cells grown on 35-mm dishes (Falcon) were infected with 10 plaque-forming units/cell of a recombinant vaccinia virus (vTF7-3) that expresses T7 RNA polymerase. Two hours later, cells were transfected with 5 μ g of plasmid DNA mixed with transfection reagent (DOTAP) according to the instructions of the manufacturer (Roche). The transfection mixture was replaced with fresh culture medium 6 h post-transfection. Cells were harvested and stored at –80 °C.

Expression of proteins in *E. coli*. Plasmids were transformed into *E. coli* strain BL21 (DE3). A single colony was grown in LB medium overnight and then diluted 100-fold in LB medium or M9 medium supplemented with 0.2% glucose. When the absorbance of the cultures reached 0.6 at 600 nm, 1 mM IPTG was added to the medium to induce protein synthesis.

At indicated times post-induction, the cell density of bacterial cultures was determined by measuring the light scattering at 600 nm.

Western blot analysis. Total protein from bacterial or HeLa cells was lysed with 2 \times SDS loading buffer (with or without 200 mM DTT) plus 10 mM of iodoacetamide and subjected to SDS-PAGE. Proteins were transferred to PVDF membrane (Stratagene) and blocked overnight at 4 °C in blocking buffer (5% fat free milk powder in TBST buffer (20 mM Tris-HCl (pH 7.4), 150 mM NaCl, and 0.1% Tween 20)). The membrane was incubated with a 1:1000 diluted primary antibody in blocking buffer for 1 h at room temperature. After washing three times with TBST, the membrane was incubated with 1:2000 diluted anti-mouse IgG conjugated with horseradish peroxidase (DAKO) in blocking buffer for 1 h at room temperature. After washing for three times with TBST, the polypeptides were detected with a chemiluminescence detection kit (ECL, Amersham Biosciences) according to the instructions of the manufacturer.

β -Galactosidase and hygromycin B assays. To measure the entry of ONPG into bacterial cells, 1 ml of bacterial cultures was removed at indicated times post-induction. After centrifugation, cells were resuspended in 1 ml of fresh M9 medium containing 2 mM ONPG, a β -galactosidase substrate. Cells were incubated for 10 min at 30 °C, and the reaction was stopped by addition of 0.4 ml of 1 M sodium carbonate. Samples were centrifuged, and the absorbance at 420 nm was measured to estimate the cleavage of ONPG.

To detect the entry of HB into bacterial cells, 1 mM of HB was added to the medium 50 min post-induction. After incubation for 30 min, 1 μ Ci of [³⁵S]methionine per ml was added to the medium and incubated at 37 °C for 15 min. The bacterial cells were then harvested and subjected to SDS-PAGE. The proteins were detected by autoradiography.

Polymerase chain reaction and site-directed mutagenesis. Amplification of the respective template DNAs with appropriate primers was performed with pfu DNA polymerase (Stratagene) under the standard buffer conditions with 2 mM MgCl₂. The PCR conditions were 35 cycles of 94 °C for 45 s, 50–58 °C for 45 s, and 72 °C for 45 s to 2 min. The annealing temperature and extension time were subjected to adjustments according to the melting temperatures of the primers used and the lengths of the PCR fragments synthesized. Site-directed mutagenesis was carried out with two rounds of PCR and two pairs of primers.

Construction of plasmids. Plasmids pET24-E, pET24-3a, pET24-3b, pET24-6, pET24-7a, and pET24-HCVE1 were constructed by cloning an *NdeI/XhoI*-digested PCR fragment into *NdeI/XhoI*-digested pET24a vector. All the constructs have a His tag fused to the 3' end of the genes. The two primers for SARS E protein are: 5'-CGGGATA TCCCATATGTA CTTCGTTTCGGAA-3' and 5'-CGGAATT CTTACTCGAGGACCAGAAGATCAGGAACTCC-3'. The two primers for SARS 3a protein are: 5'-CGGGATATCCCATATGGA TTTGTTTATGAGATTT-3' and 5'-CGGAATTCTTACTCGAGC AAAGGC-ACGCTAGTAGTTCGT-3'. The two primers for SARS 3b protein are: 5'-CGGGATATCCCATATGATGCCAACTACTT TGTTT-3' and 5'-CGGAATTCTTACTCGAGACGTACCTGTTT CTTCCGAA-A-3'. The two primers for SARS 6 protein are: 5'-CGGGATATCCCATATGTTTCTTGTGACTTC-3' and 5'-CGGAATTCTTACTCGAGTGGATAATCTAATCCATAGG-3'. The two primers for SARS 7a protein are: 5'-CGGGATATCCCAT ATGAAAATTATTCTTCTTCCTG-3' and 5'-CGGAATTCTTACT CGAGTCTGTCTTTCTTAAATGGT-3'. The two primers for HCV E1 protein are: 5'-CGGGATATCCCATATGTACCAAGTGC GCAATTCCTCG-3' and 5'-CCGGAATTCTTAGCGGCCGCCG GTCCAGCCCGCAAATAG-3'.

Plasmid pFlagE was constructed by cloning an *EcoRV*- and *EcoRI*-digested PCR fragment into *EcoRV*- and *EcoRI*-digested pFlag. The Flag tag is fused to the N-terminal end of the E protein. The two primers used are: 5'-CGGGATATCCCATATGTATCA TCGTTTCGGAA-3' and 5'-CGGAATTCTTACTCGAGGACC AGAAGATCAGGAACTCC-3'.

Results and discussion

Retardation of bacterial growth by SARS-CoV E, 6, and 7a proteins

The effect of overexpression of several SARS-CoV proteins containing potential transmembrane domain on bacterial growth was initially tested. For this purpose, nucleotide sequences covering the SARS-CoV E, 3a, 3b, 6, and 7a proteins and HCV E1 protein, respectively, were cloned into pET24a vector, and were expressed in *E. coli* BL21 (DE3), a strain carrying integrated in the chromosome the T7 RNA polymerase gene under the control of a lac UV5 promoter that can be induced by IPTG. HCV E1 protein was chosen as a positive control, as it has been shown to be able to increase membrane permeability when overexpressed in *E. coli* cells [5]. As shown in Fig. 1A, expression of 3a and 3b proteins rendered no obvious effects on the growth of bacteria, compared with bacterial cells carrying the empty plasmid pET24a. Certain degrees of retardation of bacterial growth were observed in cells expressing the E, 6, and 7a and HCV E1 proteins (Fig. 1A).

The expression of these proteins was then checked by labeling bacterial proteins with [³⁵S]methionine in the presence of rifampicin. Fig. 1B shows the presence of protein bands with apparent molecular masses of 9.3 (lane 1), 32 (lane 2), 18.5 (lane 3), 14.8 (lane 5), and 21.7 kDa (lane 6), corresponding to the expected His-tagged E, 3a, 3b, and 7a and HCV E1 proteins, respectively. However, no band corresponding to the His-tagged protein 6 (8.5 kDa) was detected (Fig. 1B, lane 4). To confirm the expression and identities of these proteins, Western blot analysis was conducted using anti-His antibody. The 9.3-kDa E protein (lane 7), 32-kDa 3a protein (lane 8), 14.8-kDa 7a protein (lane 11), and 21.7-kDa HCV E1 protein (lane 12) were detected, confirming the expression of these proteins. However, the antibody fails to react with the 3b protein (Fig. 1B, lane 9). The reason for the failure to detect the His-tagged 3b protein is currently uncertain. Once again, no obvious band corresponding to protein 6 was detected (Fig. 1B, lane 10), indicating the expression of this protein at a very low level in the bacterial cells. As significant inhibition of the growth of bacterial cells carrying this gene was observed (Fig. 1A), it suggests that the protein may be highly toxic to bacte-

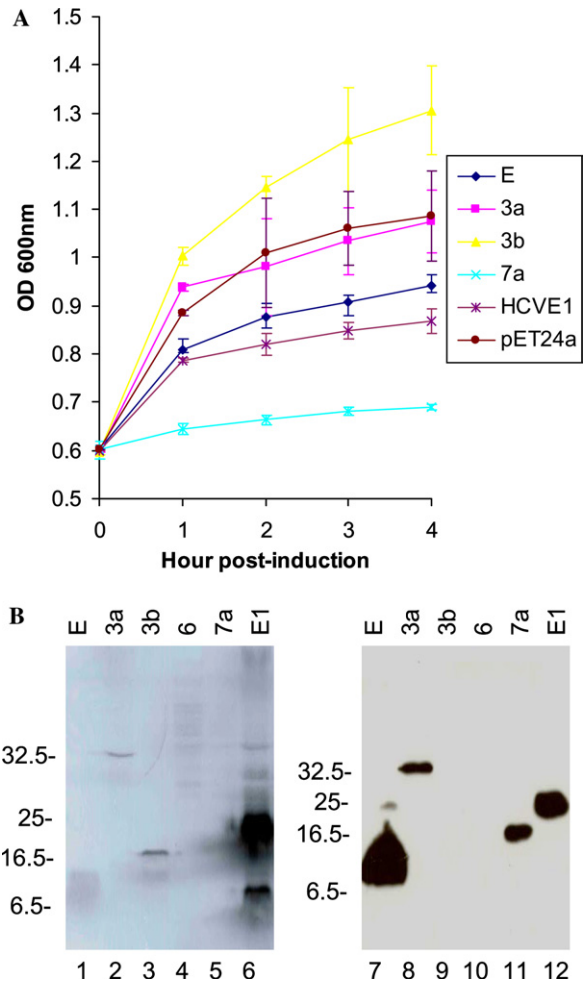


Fig. 1. (A) Effects of expression of SARS-CoV proteins on bacterial growth. *E. coli* strain BL21 (DE3) cells carrying pET24a-E, pET24a-3a, pET24a-3b, pET24a-6, pET24a-7a, pET24a-HCVE1, and pET24a were induced with 1 mM IPTG. The cell densities were measured at 600 nm at indicated times post-induction. Cells carrying pET24a-HCVE1 were used as positive control, and cells carrying pET24a were used as negative control. (B) Analysis of the expression of SARS-CoV proteins. Bacterial cells carrying plasmid pET24a-E, pET24a-3a, pET24a-3b, pET24a-6, pET24a-7a, and pET24a-HCVE1 were induced with 1 mM IPTG. To detect the protein expression directly, 150 μ g/ml of rifampicin was added 30 min post-induction. After incubation for 2 h, cells were labeled with [³⁵S]methionine for 15 min. Electrophoresis of cell extracts was carried out in SDS-15% polyacrylamide gels (lanes 1–6). The expression of these proteins from unlabeled bacterial cells harvested at 2 h post-induction was analyzed by Western blotting using anti-His monoclonal antibody (lanes 7–12). Numbers on the left indicate molecular masses in kilodaltons.

ria. This protein was excluded in the subsequent studies. It was also noted that induction of the empty vector, pET24a, affects the growth of bacteria carrying the plasmid, compared with bacteria carrying pET24a-3a and pET24a-3b (Fig. 1A). This may reflect the fact that overexpression of the multiple cloning site-His tag region in pET24a might affect bacterial growth.

Modification of membrane permeability by the expression of E protein

To test if the observed inhibition of bacterial growth by the expression of E and 7a proteins is caused by the modification of membrane permeability, HB, an antibiotic which can inhibit host cell protein synthesis but is normally impermeable to cells within a short period of time, was added to the culture medium after induction of protein expression with IPTG. When the cell membrane permeability is altered, it can translocate into cells to block cellular protein translation. Cells were metabolically labeled with [³⁵S]methionine for 15 min after addition of HB. Expression of SARS-CoV E protein allows the entry of HB to cells, as host protein synthesis was completely blocked (Fig. 2A, lanes 1 and 2). Similar inhibitory effect on host protein synthesis was observed in bacterial cells expressing the positive control protein, HCV E1 protein (Fig. 2A, lanes 5 and 6). No obvious effect on membrane permeability was observed in cells expressing 7a protein (Fig. 2A, lanes 3 and 4).

To further confirm the observation that expression of SARS-CoV E protein can induce changes in membrane permeability, entry of ONPG into bacterial cells was analyzed. ONPG, a substrate of β -galactosidase, is normally excluded by the membrane of intact cells. Entry of ONPG into bacterial cells was easily monitored by measuring its conversion to a colored compound by the β -galactosidase activity present in bacterial cells. As shown in Fig. 2B, induction of the expression of E pro-

tein caused a clear increase in the entry of ONPG into cells. These results confirm that expression of SARS-CoV E protein could increase membrane permeability in bacterial cells.

Oligomerization of E protein

We next tested if E protein could form oligomers by analysis of the E protein expressed in bacteria and mammalian cells on both reducing and non-reducing SDS-PAGE gels. After induction with IPTG, the bacterial cells were harvested and lysed with the protein loading buffer plus 10 mM of iodoacetamide to irreversibly block the free cysteinyl thiols to form disulfide bonds. Under such conditions, electrophoresis of the bacterially expressed E protein on reducing SDS-PAGE gel showed the detection of a 9.3 kDa band, representing the monomer of the E protein (Fig. 3, lane 2). In addition to the 9.3-kDa protein band, analysis of the same sample on non-reducing SDS-PAGE gel showed the detection of a protein band migrating at the position of 27 kDa (Fig. 3, lane 1), representing a putative homotrimer of the E protein.

The E protein was then expressed in HeLa cells. To detect the protein expression, an 11-amino-acid Flag tag was fused to the N-terminus of the E protein. Analysis of the E protein expressed in HeLa cell on reducing SDS-PAGE gel showed the detection of the 9.3-kDa monomer (Fig. 3, lane 4). Both the 9.3-kDa monomer and the 27-kDa trimer were observed under non-reducing conditions (Fig. 3, lane 3).

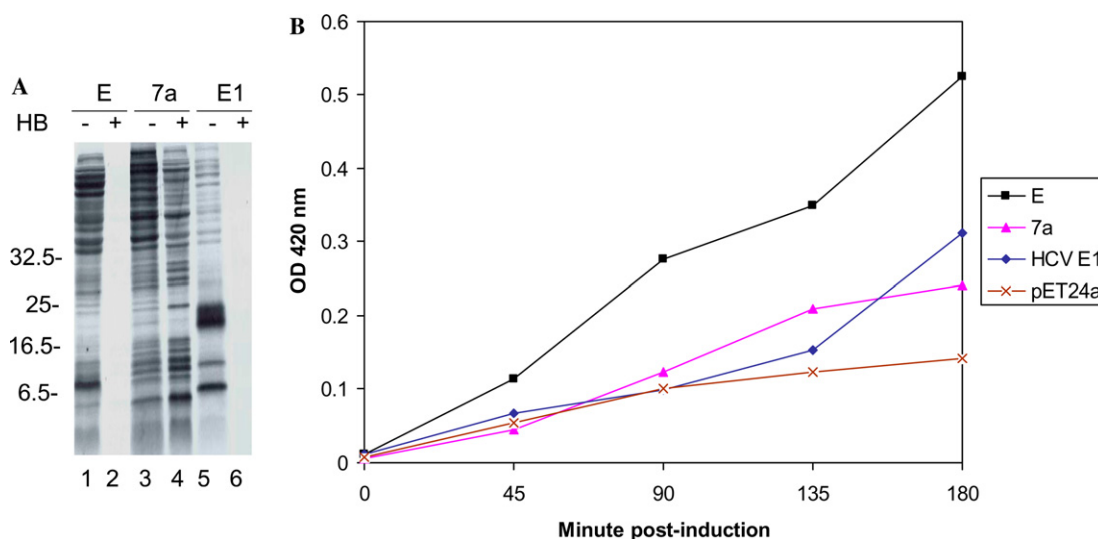


Fig. 2. Modification of membrane permeability by SARS-CoV E protein. (A) Entry of HB into bacterial cells. BL21 (DE3) cells transformed with pET24-E, pET24-7a, and pET24-HCVE1 were induced with 1 mM IPTG. At 1 h post induction, 2 mM HB was added. After incubation for 15 min, proteins were metabolically labeled with [³⁵S]methionine for 15 min. Cell extracts were analyzed by SDS-15% PAGE. Cells carrying pET24-HCVE1 were used as positive control. Numbers on the left indicate molecular masses in kiloDaltons. (B) Entry of ONPG into bacterial cells. BL21 (DE3) cells carrying pET24-E, pET24-7a, pET24-HCVE1, and pET24a were induced with 1 mM IPTG. Two millimolar ONPG was added at the indicated times and incubated at 30 °C for 10 min. The β -galactosidase activity was determined by measuring the absorbance at 420 nm. Cells carrying pET24-HCVE1 were used as positive control and cells carrying pET24a were used as negative control.

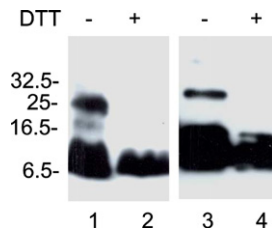


Fig. 3. Oligomerization of SARS-CoV E protein. The His-tagged E protein expressed in bacteria (lanes 1 and 2) and the flag-tagged E protein expressed in HeLa cells were separated on SDS–15% polyacrylamide gels under reducing (lanes 2 and 4) and non-reducing (lanes 1 and 3) conditions. Polypeptides were transferred to PVDF membrane and probed with anti-His (lanes 1 and 2) and anti-Flag (lanes 3 and 4) monoclonal antibodies, respectively. After incubation with horseradish peroxidase-conjugated anti-mouse IgG, the E protein was detected by a chemiluminescence detection kit. Numbers on the left indicate molecular masses in kiloDaltons.

Occasionally, a protein band migrating between the 9.3-kDa monomer and the 27-kDa trimer could be detected when the E protein expressed in both bacterial and mammalian cells was analyzed under non-reducing conditions (Fig. 3, lanes 1 and 3; and see Fig. 4B). It may represent dimerization of the E protein. These results suggest that the E protein may form homo-dimers and trimers in both bacterial and mammalian cells.

The essential roles of two cysteine residues of E protein in its modification of membrane permeability and oligomerization in E. coli cells

Examination of the amino acid sequence of E protein showed that the protein contains three cysteine residues at amino acid positions 40 (C1), 43 (C2), and 44 (C3), respectively. To analyze the involvement of these cysteine residues in the oligomerization of E protein, site-directed mutagenesis of these cysteine residues to alanine either individually or in combination of two or three was made to generate five mutants (M1–M5). Mutant M1 contains mutation at the C1 position, M2 at C2, and M3 at C3. M4 contains mutations at both the C1 and C2 positions, and M5 contains mutations at all three positions. These mutants were then expressed in *E. coli* BL21 (DE3). As can be seen in Fig. 4A, expression of wild type E protein and mutant M2 showed obvious induction of membrane permeability, as significant inhibition of protein synthesis by HB was observed (lanes 1 and 2; and lanes 5 and 6). Expression of mutants M1, M3, M4, and M5 showed no obvious increase of membrane permeability to HB (Fig. 4A, lanes 3, 4, and 7–12), indicating that these mutations may abolish the function of E protein in its induction of membrane permeability in bacterial cells. These results demonstrate that C1 and C3 residues are crucial for the function of E protein.

Analysis of the expression of wild type and mutant E protein was then carried out to see if the two cysteine

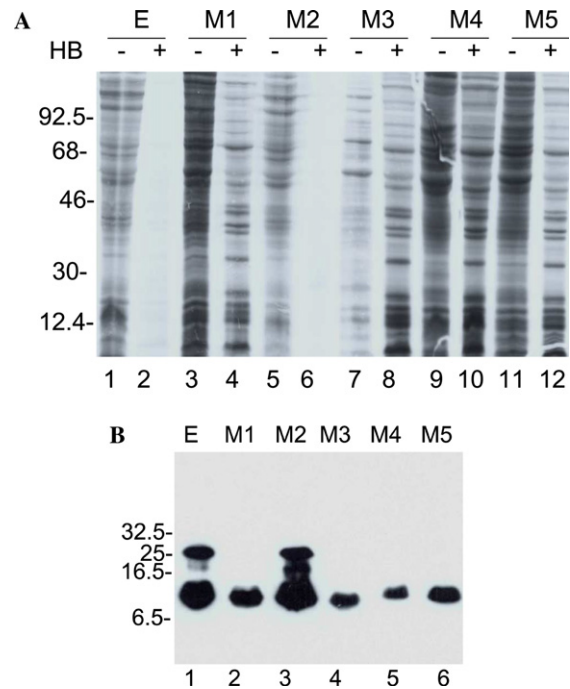


Fig. 4. Mutational analysis of the role of three cysteine residues of E protein in its modification of membrane permeability and oligomerization. (A) Entry of HB into bacterial cells expressing wild type and mutant E proteins. BL21 (DE3) cells transformed with pET24-E, pET24-M1, pET24-M2, pET24-M3, pET24-M4, and pET24-M5 were induced with 1 mM IPTG. At 1 h post-induction, 2 mM HB was added. After incubation for 15 min, proteins were metabolically labeled with [³⁵S]methionine for 15 min. Cell extracts were analyzed by SDS–15% polyacrylamide gel. Numbers on the left indicate molecular mass in kiloDaltons. (B) Oligomerization of wild type and mutant E protein. The His-tagged wild type and mutant E proteins expressed in BL21 (DE3) were separated on SDS–15% polyacrylamide gels under non-reducing conditions. Polypeptides were transferred to PVDF membrane and probed with anti-His monoclonal antibody. After incubation with horseradish peroxidase-conjugated anti-mouse IgG, the E protein was detected by a chemiluminescence detection kit. Numbers on the left indicate molecular masses in kiloDaltons.

residues are involved in the formation of the oligomers. As shown in Fig. 4B, both the 9.3-kDa monomer and the 27-kDa homotrimer were detected in bacterial cells expressing wild type E protein and M2 under non-reducing conditions (lanes 1 and 3). Only the 9.3-kDa monomer was detected in bacterial cells expressing M1, M3, M4, and M5 under the same non-reducing conditions (Fig. 4B, lanes 2, 4, 5, and 6). As mentioned, a protein band of approximately 18 kDa migrating between the 9.3-kDa monomer and the 27-kDa homotrimer was detected in cells expressing both wild type E protein and M2 (Fig. 4B, lanes 1 and 3). These results confirm that the two cysteine residues are involved in oligomerization of the E protein by formation of interchain disulfide bonds.

Cytolytic animal viruses encode small hydrophobic integral membrane proteins to modify host cell membrane permeability during their infection cycles. These

proteins contain at least one transmembrane domain that interacts with and expands the lipid bilayer, and could form hydrophilic pores in the membrane by oligomerization, with hydrophilic residues presumably facing the aqueous lumen of the pore [4,7]. The hydrophilic channels would allow low molecular weight hydrophilic molecules across the membrane barrier, leading to the disruption of membrane potential, collapse of ionic gradients, and release of essential compounds from the cell. Alterations in ion concentration, such as enhancing the intracellular concentration of sodium ions, in the cytoplasm of virus-infected cells at the beginning of viral protein synthesis would favor virus replication. This would promote translation of viral versus cellular mRNAs, as translation of mRNAs from many cytolitic animal viruses is fairly resistant to high sodium concentrations. In contrast, high sodium concentrations are inhibitory to the translation of most cellular mRNAs [4,7]. Progressive membrane damage during viral replication cycles would also result in cell lysis, promote virus release, and facilitate virus spread to surrounding cells. Disruption of the function of viroporins would therefore abrogate viral infectivity, rendering this group of viral proteins suitable targets for the development of antiviral drugs.

Is the SARS-CoV E protein a viroporin? Data presented in this study demonstrated that expression of E protein in bacteria inhibits bacterial growth, increase the entry of ONPG and HB into bacterial cells. Furthermore, the protein could form homo-dimers and trimers by interchain disulfide bonds in both bacterial and mammalian cells. These observations support that SARS-CoV E protein might function as a viroporin. Further studies are required to address if similar modification of membrane permeability can be observed in other systems, including yeast and mammalian cells.

Coronavirus E protein is a minor virion component [14]. It plays an essential role in virion assembly and morphogenesis [12]. Computer-aided programs predict that SARS-CoV E protein may contain a putative α -helical transmembrane domain from amino acids 11–33. Similar to other viroporins, SARS-CoV E protein also contains some hydrophilic residues in the helical region. These functional and structural features resemble the influenza virus M2 protein, the best characterized ion-channel forming viroporin with four α -helices and a tetrameric quaternary structure [17]. If the SARS-CoV E protein were proved to be able to form ion channels in cellular membranes, it would open a way to design anti-SARS therapeutic approaches.

Is induction of membrane permeability a general feature of coronavirus E protein? Although the E proteins from different coronaviruses share a low homology in their primary amino acid sequences, the general structural features consisting of an α -helical transmembrane domain are conserved. It suggests that the E protein may play very similar roles, including induction of host

cell membrane permeability changes critical for the replication of coronaviruses. Comparative studies of E proteins from different coronavirus would help delineate the molecular and structural basis of their modification of membrane permeability and potential pore-forming activities.

Acknowledgments

This work was supported by grants from Nanyang Technological University (SUG15/02) and from the Biomedical Research Council (BMRC 03/1/22/17/220), Agency for Science Technology and Research, Singapore.

References

- [1] A. Agirre, A. Barco, L. Carrasco, J.B. Nieva, Viroporin-mediated membrane permeabilization, *J. Biol. Chem.* 277 (2002) 40434–40441.
- [2] R. Aldabe, A. Barco, L. Corrasco, Membrane permeabilization by poliovirus proteins 2B and 2BC, *J. Biol. Chem.* 271 (1996) 23134–23137.
- [3] G. Bodelon, L. Labrada, J. Martinez-Costas, J. Benavente, Modification of late membrane permeability in avian reovirus-infected cells, *J. Biol. Chem.* 227 (2002) 17789–17796.
- [4] L. Carrasco, L. Perez, A. Irurzun, J. Lama, F. Martinez-Abarca, P. Rodriguez, R. Guinea, J.L. Castrillo, M.A. Sanz, M.J. Ayala, Modification of membrane permeability by animal viruses, *Adv. Virus Res.* 45 (1995) 61–112.
- [5] A.R. Ciccaglione, C. Marcantonio, A. Costantino, M. Equestre, A. Geraci, M. Rapietta, Hepatitis C virus E1 protein induces modification of membrane permeability in *E. coli* cells, *Virology* 250 (1998) 1–8.
- [6] M.E. Gonzalez, L. Carrasco, The human immunodeficiency virus type 1 vpu protein enhances membrane permeability, *Biochemistry* 37 (1998) 13710–13719.
- [7] M.E. Gonzalez, L. Carrasco, Viroporins, *FEBS Lett.* 552 (2003) 28–34.
- [8] S.D.C. Griffin, L.P. Beales, D.S. Clarke, O. Worsfold, S.D. Evans, J. Jaeger, M.P.G. Harris, D.J. Rowlands, The p7 protein of hepatitis C virus forms an ion channel that is blocked by the antiviral drug, Amantadine, *FEBS* 535 (2003) 34–38.
- [9] T.G. Ksiazek, D. Erdman, C.S. Goldsmith, S.R. Zaki, T. Peret, S. Emery, S. Tong, C. Urbani, J.A. Comer, W. Lim, P.E. Rollin, S.F. Dowell, A.E. Ling, C.D. Humphrey, W.J. Shieh, J. Guarner, C.D. Paddock, P. Rota, B. Fields, J. DeRisi, J.Y. Yang, N. Cox, J.M. Hughes, J.W. LeDuc, W.J. Bellini, L.J. Anderson and SARS Working Group, A novel coronavirus associated with severe acute respiratory syndrome, *N. Engl. J. Med.* 348 (2003) 1953–1966.
- [10] M. Jecht, C. Probst, V. Gauss-Muller, Membrane permeability induced by Hepatitis A virus proteins 2B and 2BC and proteolytic processing of HAV 2BC, *Virology* 252 (1998) 218–227.
- [11] J. Lama, L. Carrasco, Expression of poliovirus nonstructural proteins in *Escherichia coli* cells, *J. Biol. Chem.* 267 (1992) 15932–15937.
- [12] K.P. Lim, D.X. Liu, The missing link in coronavirus assembly, *J. Biol. Chem.* 276 (2001) 17515–17523.
- [13] C. Liu, H.Y. Xu, D.X. Liu, Induction of caspase-dependent apoptosis in cultured cells by the avian coronavirus infectious bronchitis virus, *J. Virol.* 75 (2001) 6402–6409.

- [14] D.X. Liu, S.C. Inglis, Association of the infectious bronchitis virus3c protein with the virion envelope, *Virology* 185 (1991) 911–917.
- [15] D. Pavlovic, D.C.A. Neville, O. Argaud, B. Blumberg, R.A. Dwek, W.B. Fischer, N. Zitzmann, The hepatitis C virus forms an ion channel that is inhibited by long-alkyl-chain iminosugar derivatives, *Proc. Natl. Acad. Sci. USA* 100 (2003) 6104–6108.
- [16] L.H. Pinto, L.J. Holsinger, R.A. Lamb, Influenza virus M2 protein has ion channel activity, *Cell* 59 (1992) 517–528.
- [17] L.H. Pinto, R.A. Lamb, viral ion channels as models for ion transport and targets for antiviral drug action, *FEBS Lett.* 560 (2004) 1–2.
- [18] P.A. Rota, M.S. Oberste, S.S. Monroe, W.A. Nix, R. Campagnoli, J.P. Icenogle, S. Penaranda, B. Bankamp, K. Maher, M.-H. Chen, S. Tong, A. Tamin, L. Lowe, M. Frace, J.L. DeRisi, Q. Chen, D. Wang, D.D. Erdman, T.C.T. Peret, C. Burns, T.G. Ksiazek, P.E. Rollin, A. Sanchez, S. Liffick, B. Holloway, J. Limor, K. McCaustland, M. Olsen-Rasmussen, R. Fouchier, S. Gunther, A.D.M.E. Osterhaus, C. Drosten, M.A. Pallansch, L.J. Anderson, W.J. Bellini, Characterization of a novel coronavirus associated with severe acute respiratory syndrome, *Science* 300 (2003) 1394–1399.
- [19] M.A. Sanz, L. Perez, L. Carrasco, Semliki forest virus 6K protein modifies membrane permeability after inducible expression in *Escherichia coli* cells, *J. Biol. Chem.* 269 (1994) 12106–12110.
- [20] V. Thiel, K.A. Ivanov, A. Putics, T. Hertzog, B. Schelle, S. Bayer, B. Weißbrich, E.J. Snijder, H. Rabenau, H.W. Doerr, A.E. Gorbalenya, J. Ziebuhr, Mechanisms and enzymes involved in SARS coronavirus genome expression, *J. Gen. Virol.* (2003).